Theoretical Computer Science 547 (2014) 90–103

Contents lists available at ScienceDirect

Theoretical Computer Science

www.elsevier.com/locate/tcs

"Robot Cloud" gradient climbing with point measurements ☆

Yotam Elor *, Alfred M. Bruckstein

Department of Computer Science and the Technion Goldstein UAV and Satellite Center, Technion, Haifa 32000, Israel

ARTICLE INFO

Article history:
Received 31 December 2012
Received in revised form 16 November 2013
Accepted 18 June 2014
Available online 26 June 2014
Communicated by D. Peleg

Keywords:
Source-seeking
Point measurement
Gradient
Fume tracking

ABSTRACT

A scalar-field gradient climbing process for a large group of simple, low-capability mobile robotic agents using only point measurements is proposed and analyzed. The agents are assumed to be memoryless and to lack direct communication abilities. Their only implicit form of communication is by sensing the position of the members of the group. The proposed gradient following algorithm is based on a basic gathering algorithm. The gathering algorithm is augmented by controlling the agents' speed as follows: agents that sense a higher value of the field move slower toward the group center than those sensing lower values, thereby causing the swarm to drift in the direction of the underlying field gradient. Furthermore, a random motion component is added to each agent in order to prevent gathering and allow sampling of the scalar field. We prove that in the proposed algorithm, the group is cohesive and indeed follows the gradient of the scalar field. We also discuss an algorithm based on a more restrictive sensing capabilities for the agents.

1. Introduction

In this work we consider the problem of designing the control for a group of robots so that they will follow the gradient of a scalar field defined over d-dimensional space $\rho : \mathbb{R}^d \to \mathbb{R}$ where $d \in \mathbb{N}$. Our claim is to have the group motion as the result of simple memoryless interactions between the robotic agents. It is often assumed that the scalar field is the concentration of some chemical material and is generated by a diffusion process originating at a source. Therefore, the value of the scalar field becomes weaker as one moves away from it. Hence, the problem is sometimes called *source-seeking* with applications varying from tracking a plume of gas to finding the source of leakage of an hazardous chemical.

A large group of miniature (possibly nano) and very simple robotic agents with very low capabilities is considered. Very small robots, even equipped with multiple sensors, are unable to directly sense the gradient of $\rho(\cdot)$, the scalar field, because the spatial separation between the on board sensors is not large enough. Hence, it is assumed that the agents can only take point measurements of $\rho(\cdot)$. We limit the discussion to *memoryless*, or *reactive*, algorithms in the sense that an action performed by an agent is determined solely by the agent's sensors readings at the time the action is taken. Since they are *memoryless*, the agents cannot estimate the gradient by comparing the currently measured value to previously sensed values and, by assumption, they cannot communicate directly thus cannot explicitly share their point measurements.

Full mutual sensing of position is assumed, i.e. every agent can sense the relative position of all other agents in the group. This assumption might seem quite strange and restrictive, however our results prove that by tuning the algorithm parameters the swarm can be made as cohesive as desired. Specifically, the swarm can be made cohesive enough to guarantee that at (almost) all times, all agent pairs are close enough to allow mutual sensing of relative position (see the discussion in Section 5). Nevertheless, some alternatives to full position sensing are explored in Section 5.1.

☆ This research was supported by the Technion Goldstein UAV and Satellite Center.

* Corresponding author.

http://dx.doi.org/10.1016/j.tcs.2014.06.025

Alternatively, as formalized in Section 4, the proposed process can be described as a gathering or swarming algorithm augmented to allow gradient climbing. The agents follow the swarming algorithm while their speed is controlled by the scalar field, or in other words, the medium they travel in. Many swarming algorithms, including those used in this work, can be employed by considering potential fields which are both induced by the agents and dictate the agents movement. Hence, instead of sensing all other agents relative positions, each agent can simply react to the potential field induced by the other agents while its speed is controlled by the local scalar field.

2. Previous work

In a recent paper we have proposed a gradient climbing algorithm for two memoryless robotic agents using only implicit communication and point measurements [1]. The two agents considered were assumed to orbit their center of mass while the agent who senses the higher ρ-value strives to maintain a slightly larger distance from the center of mass. As a result, the robot pair was shown to drift toward higher ρ-values. The algorithm proposed here may be viewed as an extension of the same basic mechanism to the multi-agent scenario.

A broad survey of previous work on gradient following by multiple agents can be found in our previous paper [1]. Hence only the most relevant work will be discussed here. With a single agent, the common method used to overcome the point measurement limitation is by taking spatially separated measurements by moving the agent between readings. By "remembering" and subsequently comparing the readings, the agent can estimate the gradient, see e.g. [2,3]. As the agent moves, the field value it measures changes. Assuming continuous measurement, the time differential of the readings ($\dot{\rho}(\cdot)$) can be recorded and used to control the agent, see e.g. [4–6]. All the above under the assumption that the agent has memory.

In a multi-agent scenario where every agent is able to measure and communicate $\rho(\cdot)$ or the gradient of $\rho(\cdot)$, variants of the Artificial Potential Field framework can be employed [7,8]. Gazi and Passino[9] studied the behavior of a swarm of agents affected by attraction, repulsion and gradient climbing forces. They proposed rules of motion ensuring that the swarm maintains cohesiveness and travels in the direction of the gradient.

An algorithm that uses point measurements only was proposed in [10]. There, N agents maintain a uniform circle formation. By comparing the values they measure, the agents in the formation move with the gradient. However, in contrast to our work, in [10] every agent is assumed to have access to the values measured by all other agents. Recently, Berdhal et al. [11] observed gradient climbing behavior in schools of fish i.e. individual fish reduce their speed when sensing low light levels resulting in movement of the school toward darker regions of the aquarium. Inspired from this work, Wu et al. formalized the algorithm of [11] and proved convergence to a peak in the scalar field. Similarly to our work, Wu et al. [12] also assume full visibility and a linear scalar field, however, their algorithm is different from ours. Recently, Wu and Zhang shown that a switching strategy i.e. the agents switch between individual exploration and cooperative exploration improve the convergence time [13].

3. Preliminaries

The environment considered in this work is the d-dimensional space $\mathbb{R}^d$. For real scenarios it is natural to consider $1 \le d \le 3$. By assumption, there is a scalar field $\rho(\cdot)$ defined over the space $\rho : \mathbb{R}^d \to \mathbb{R}$. The agents' task is to follow the gradient of $\rho(\cdot)$. The system comprises $M \ge 2$ agents denoted by $r_1..r_M$. The location of agent r_i in a fixed global coordinate frame is given by X_i where

$$X_i = \left[x_i^1, x_i^2 ... x_i^d\right]^T \tag{1}$$

The unit vectors of the global coordinate system are denoted by $\hat{x}^1 ... \hat{x}^d$. Note that the global coordinate frame is unknown to the agents and is defined here solely for convenience of analysis. Let X_{cm} be the agents' center of mass, which, in the global coordinate system, is given by

$$X_{cm} = \frac{1}{M}\sum_{i=1}^{M} X_i \tag{2}$$

Let $\rho(X)$ denote the value of the scalar field at point X.

In our model time is discrete, i.e. $t = 0, 1, 2....$ It is assumed that the algorithm was initialized at time $t = 0$. When we explicitly add t to the indices of a quantity we refer to the value of that quantity at time t, e.g. $X_i(t)$ is the location of agent r_i at time t.

4. Gradient-climbing process

Consider the following function, the sum of all squared inter-robot distances

$$\Psi\{X_1, X_2 ... X_M\} \triangleq \frac{1}{2}\sum_{i,j} d(X_i, X_j)^2 \tag{3}$$

where $d(p,q)$ is the Euclidean distance between points p and q. Note that Ψ is induced by all agents. A natural gathering algorithm is given by the following gradient descent process in which every agent follows the local gradient of $-a\Psi$:

$$\frac{\partial X_i}{\partial t} \triangleq -a\frac{\partial \Psi}{\partial X_i} = a\sum_{j=1}^{M}(X_j - X_i) \tag{4}$$

where a is a small positive constant. One can easily show that Ψ decreases under the rule of motion above thus the swarm gathers. In Eq. (4) the motion vector of every agent is the sum of the position difference vectors toward all other agents. A different interpretation is seen by presenting Eq. (4) in the following manner:

$$\frac{\partial X_i}{\partial t} = Ma(X_{cm} - X_i) \tag{5}$$

i.e., every agent in fact moves toward the group's instantaneous center of mass and the agent's speed is proportional to the distance to the center of mass. It is also readily seen that the center of mass remains stationary, unaffected by the motion of the robots toward it. Cohen and Peleg studied similar gathering algorithms under a different robot model, see [14].

We propose to augment the gathering algorithm above in order to ensure gradient climbing behavior by replacing the constant speed a with a non-constant function determined by the local point measurement taken by each agent. We shall do this by simply causing agents who sense high ρ-values move toward the center of mass slightly slower than agents who sense lower values. We shall prove below that such a simple modification of the basic gathering process, along with a randomization step that effectively avoids collapse of the swarm to a single point, will cause the swarm to drift in the direction of the gradient.

By augmenting the rule of Eq. (4) as described above and discretizing time we get the following local rule of motion, to be executed by every agent r_i at every time step t:

$$X_i(t+1) = X_i(t) + R_i(t) + \big(1-\alpha-\beta\rho(X_i)\big)\frac{1}{M}\sum_{j=0}^{M}\big(X_j(t) - X_i(t)\big) \tag{6}$$

$$= X_i(t) + R_i(t) + \big(1-\alpha-\beta\rho(X_i)\big)\big(X_{cm}(t) - X_i(t)\big) \tag{7}$$

where α and β are constants chosen so that $0 < \alpha < \frac{1}{2}$, $0 < \beta < (1-2\alpha)/\rho_{\max}$. Here $R_i(t)$ is the random step taken by agent i at time t. For any agent r_i and time t, $R_i(t)$ is distributed as a d-dimensional Gaussian with zero mean and covariance matrix $I \cdot \sigma_R^2$ where σ_R^2 is a positive constant. The components of $R_i(t)$ are denoted by $R_i^1(t) \ldots R_i^d(t)$ and each is normally distributed with zero mean and variance σ_R^2 independently of all other random variables in the system.

4.1. Drift analysis

The analysis provided in this section holds for $M \geq 2$ agents. The algorithm is analyzed under the assumption that the gradient of the scalar field is constant in the neighborhood spanned by the agents. This assumption is justified by noting that a cohesive swarm may indeed occupy a relatively small portion of space. It is reasonable to assume that the gradient of $\rho(\cdot)$ will be roughly constant in such a small portion of space. Extensive simulations with complex and noisy scalar fields were conducted in order to show that the group of agents performs gradient ascent even when the gradient is not constant, see Section 5.

Without loss of generality, for environments of any dimension, we shall consider that the field $\rho(\cdot)$ is linear having the gradient in the x^1-direction, i.e. $\rho(X_i) = \rho_0 \cdot x_i^1$ where ρ_0 is a small positive constant ($0 < \rho_0 \ll 1$). The gradient field is then constant as given by $\nabla\rho = \rho_0 \hat{x}^1$. Note that Eq. (7) is invariant under Euclidean transformation of $\mathbb{R}^d$, hence for the analysis purpose we can indeed select the x^1-axis to coincide with the gradient of $\rho(\cdot)$. It is further assumed that the scalar field $\rho(\cdot)$ is bounded by $0 \leq \rho(\cdot) \leq \rho_{\max}$ where $\rho_{\max}$ is a known upper bound. Note that in an infinite space with constant gradient the value of $\rho(\cdot)$ can not be bounded. However, in practice, $\rho(\cdot)$ must have an upper bound – even one only resulting from the limits of the sensor. So having an upper bound on $\rho(.)$ is a reasonable assumption.

Recall that $x_i^j(t)$ is the j'th coordinate of the location of agent r_i in the global coordinate frame at time t. By substitution of $\rho(X_i) = \rho_0 x_i^1$ into Eq. (7) we get for each coordinate j, $1 \leq j \leq d$,

$$x_i^j(t+1) = x_i^j(t) + R_i^j(t) + \big(1-\alpha-\beta\rho_0 x_i^1(t)\big)\big(x_{cm}^j(t) - x_i^j(t)\big) \tag{8}$$

Thus we have a set of stochastic coupled difference equations. Note, however, that due to the choice of the frame of coordinates to have the gradient in the direction of $\hat{x}^1$, the recursive equations for the first component of the robotic agent coordinates ($j = 1$) are independent of the other coordinates. Hence, we start the analysis by characterizing the set of solutions for the first coordinate of the recursive equation.

Lemma 1. *For any $t \geq 0$, assuming $x_1^1(t) \ldots x_M^1(t)$ are known,*

$$E_{R(t)}\left[x_{cm}^1(t+1)\right] = x_{cm}^1(t) + \beta\rho_0 SV\left[x^1(t)\right] \tag{9}$$

$$SV\left[x^1(t)\right] = \frac{1}{M}\sum_{i=1}^{M}\left(x_i^1(t) - x_{cm}^1(t)\right)^2 \tag{10}$$

where $E_{R(t)}[\cdot]$ represents expectation over all random steps taken at time step t.

Proof. By Eq. (8),

$$\begin{aligned} E\left[x_{cm}^1(t+1)\right] &= E\left[\frac{1}{M}\sum_{i=1}^{M} x_i^1(t+1)\right] && (11)\\ &= E\left[\frac{1}{M}\sum_{i=1}^{M}\left(x_i^1(t) + R_i^1(t) + \left(1 - \alpha - \beta\rho_0 x_i^1(t)\right)\left(x_{cm}^1(t) - x_i^1(t)\right)\right)\right] && (12)\\ &= x_{cm}^1(t) + \frac{\beta\rho_0}{M}\sum_{i=1}^{M} x_i^1(t)\left(x_i^1(t) - x_{cm}^1(t)\right) && (13)\\ &= x_{cm}^1(t) + \beta\rho_0 SV\left[x^1(t)\right] && (14) \end{aligned}$$

where we have used $E[R_i^1(t)] = 0$. □

By Lemma 1 the speed of the first coordinate of the center of mass is proportional to $SV[x^1(t)]$, the sample variance of the first coordinates of the agents. We can not predict that sample variance accurately. Nevertheless, a lower bound on the expected value of $SV[x^1(t)]$ is provided by the following lemma.

Lemma 2. *For any t,*

$$E_{x_1^1(t)\ldots x_M^1(t)}\left[SV\left[x^1(t)\right]\right] \geq \frac{1}{M}\sum_{i=1}^{M} Var\left[x_i^1(t)\right] \geq \sigma_R^2 \tag{15}$$

where $E_{x_1^1(t)\ldots x_M^1(t)}[\cdot]$ represents expectation over the first coordinate of the agents at time t and $Var[x_i^1(t)]$ is the variance of the random variable $x_i^1(t)$.

Proof. Consider $x_1^1(t) \ldots x_M^1(t)$ as random variables and note that $x_{cm}^1(t)$ is a random variable statistically dependent on the set $x_1^1(t) \ldots x_M^1(t)$. For each random variable $x_i^1(t)$, $E[x_i^1(t)]$ is the minimizer of the function $f(x) = E_{x_i^1(t)}[(x_i^1(t) - x)^2]$. Hence for any $x_{cm}^1(t)$ we have

$$E_{x_i^1(t)}\left[\left(x_i^1(t) - E\left[x_i^1(t)\right]\right)^2\right] \leq E_{x_i^1(t)}\left[\left(x_i^1(t) - x_{cm}^1(t)\right)^2\right] \tag{16}$$

To prove the left inequality of Eq. (15) we write,

$$\begin{aligned} E_{x_1^1(t)\ldots x_M^1(t)}\left[SV\left[x^1(t)\right]\right] &= \frac{1}{M} E_{x_1^1(t)\ldots x_M^1(t)}\left[\sum_{i=1}^{M}\left(x_i^1(t) - x_{cm}^1(t)\right)^2\right] && (17)\\ &\geq \frac{1}{M} E_{x_1^1(t)\ldots x_M^1(t)}\left[\sum_{i=1}^{M}\left(x_i^1(t) - E\left[x_i^1(t)\right]\right)^2\right] && (18)\\ &= \frac{1}{M}\sum_{i=1}^{M} E_{x_i^1(t)}\left[\left(x_i^1(t) - E\left[x_i^1(t)\right]\right)^2\right] && (19)\\ &= \frac{1}{M}\sum_{i=1}^{M} Var\left[x_i^1(t)\right] && (20) \end{aligned}$$

To prove the right inequality of Eq. (15) recall that by Eq. (8), $x_i^1(t)$ is a sum of two independent random variables: $R_1(t-1)$ and $x_i^j(t) + (1 - \alpha - \beta\rho_0 x_i^1(t))(x_{cm}^j(t) - x_i^j(t))$ hence

$$Var\big[x_i^1(t)\big] = Var\big[R_i^1(t-1)\big] + Var\big[x_i^j(t) + \big(1-\alpha-\beta\rho_0 x_i^1(t)\big)\big(x_{cm}^j(t) - x_i^j(t)\big)\big] \tag{21}$$

$$\geq Var\big[R_i^1(t-1)\big] = \sigma_R^2. \qquad \square \tag{22}$$

The bound provided in Lemma 2 is not tight. In Section 4.2, a better prediction of $SV[x^1(t)]$ is derived using two reasonable simplifying assumptions. By Lemmas 1 and 2, the agents' center of mass drifts with the gradient faster than $\beta\rho_0\sigma_R^2$. In the rest of the proof we shall show that the swarm does not drift in directions perpendicular to the gradient.

Since Eq. (8) the path of every agent is a stochastic process with infinitely many realizations and every realization has a certain probability of occurrence. Let $x_i^1(0)$,$x_i^1(1)$...$x_i^1(t-1)$ be the first t elements of a realization to the $j=1$ component of Eq. (8). Such a partial realization of Eq. (8) is "sample-path" since it is an admissible solution to the equation. Similarly, we will use *sample-paths* for x_{cm}^j i.e. we will assume that $x_{cm}^1(0)$,$x_{cm}^1(1)$...$x_{cm}^1(t-1)$ is a specific partial realization of Eq. (8).

For $2 \leq j \leq d$, denote the probability distribution function of $x_i^j(t)$ by $f_{x_i^j}(x;t)$ i.e. $f_{x_i^j}(x;t) = Pr[x_i^j(t) = x]$. The characteristic function of a probability distribution function $f_x(x)$ is defined by $\varphi_x(s) = E[e^{isx}]$. The next lemma provides the characteristic function $\varphi_{x_i^j}(x;t+1)$ for any $t \geq 0$ assuming the *sample-paths* $x_i^1(0)\ldots x_i^1(t)$ and $x_{cm}^j(0)\ldots x_{cm}^j(t)$ are given.

Lemma 3. *For any agent r_i, $2 \leq j \leq d$, $t \geq 0$, given the initial distribution $f_{x_i^j}(x;0)$ and* sample-paths $x_i^1(0)\ldots x_i^1(t)$, $x_{cm}^j(0)\ldots x_{cm}^j(t)$, *the characteristic function of $f_{x_i^j}(x;t+1)$ is given by*

$$\varphi_{x_i^j}(s;t+1) = \varphi_{x_i^j}\big(\gamma(0,t)\cdot s;0\big)\cdot \prod_{t'=0}^{t} \exp\left\{\frac{1}{2}\sigma_R^2\gamma^2\big(t'+1,t\big)s^2\right\}$$

$$\cdot \prod_{t'=0}^{t} \exp\big\{i\gamma\big(t'+1,t\big)s\big(1-\alpha-\beta\rho_0 x_i^1\big(t'\big)\big)x_{cm}^j\big(t'\big)\big\} \tag{23}$$

where

$$\gamma(t_1,t_2) = \begin{cases} \prod_{t'=t_1}^{t_2}(\alpha+\beta\rho_0 x_i^1(t')) & t_2 \geq t_1 \\ 1 & else. \end{cases} \tag{24}$$

Proof. The proof is by induction on t. The induction base can be proved by substitution of $t=0$ into Eq. (23). To prove the induction step, assume that Eq. (23) holds for any $t' \leq t$. When considering $x_i^1(t)$ and $x_{cm}^j(t)$ to be known constants, Eq. (8) implies the following recursive equation for the probability distribution function $f_{x_i^j}(x;t+1)$,

$$f_{x_i^j}(x;t+1) = \delta\big(x-\big(1-\alpha-\beta\rho_0 x_i^1(t)\big)x_{cm}^j(t)\big) * f_R(x;t) * f_{x_i^j}\left(\frac{x}{\alpha+\beta\rho_0 x_i^1(t)};t\right) \tag{25}$$

where $*$ represents one dimensional convolution and $f_R(x;t)$ is the probability distribution function of $R_i^j(t)$. The analogous recursive equation for the characteristic function $\varphi_{x_i^j}(x;t+1)$ is given by

$$\varphi_{x_i^j}(s;t+1) = \int_{-\infty}^{\infty} e^{isx} f_{x_i^j}(x;t+1)dx \tag{26}$$

$$= \left[\int_{-\infty}^{\infty} e^{isx} f_{x_i^j}\left(\frac{x}{\alpha+\beta\rho_0 x_i^1(t)};t\right)dx\right]\cdot\varphi_R(s;t)\cdot\varphi_\delta(s;t) \tag{27}$$

$$= \left[\int_{-\infty}^{\infty} e^{is(\alpha+\beta\rho_0 x_i^1 t)x'} f_{x_i^j}\big(x';t1\big)dx'\right]\cdot\varphi_R(s;t1)\cdot\varphi_\delta(s;t) \tag{28}$$

$$= \varphi_{x_i^j}\big(\big(\alpha+\beta\rho_0 x_i^1 t\big)s;t\big)\cdot\varphi_R(s;t)\cdot\varphi_\delta(s;t) \tag{29}$$

where $x' = x/(\alpha+\beta\rho_0 x_i^1(t))$; $\varphi_R(s;t) = \exp\{\frac{1}{2}\sigma_R^2 s^2\}$ is the characteristic function of $f_R(x;t)$; and $\varphi_\delta(s;t) = \exp\{is(1-\alpha-\beta\rho_0 x_i^1(t))x_{cm}^j(t)\}$ is the characteristic function of $\delta(x-(1-\alpha-\beta\rho_0 x_i^1(t))x_{cm}^j(t))$. Substitution of the induction hypothesis into the equation above yields

$$\varphi_{x_i^j}(s;t+1)=\varphi_{x_i^j}\left(\left[\prod_{t'=0}^{t}(\alpha+\beta\rho_0x_i^1(t'))\right]\cdot s;0\right)\cdot\prod_{t'=0}^{t}\varphi_R\left(\left[\prod_{t''=t'+1}^{t}(\alpha+\beta\rho_0x_i^1(t''))\right]s;t'\right)$$
$$\cdot\prod_{t'=0}^{t}\varphi_\delta\left(\left[\prod_{t''=t'+1}^{t}(\alpha+\beta\rho_0x_i^1(t''))\right]s;t'\right) \tag{30}$$

concluding the proof. □

The following lemma shows that for large enough t, the j'th coordinate of every agent, where $2\le j\le d$, is distributed normally. The mean and variance of the distribution are determined by the "sample path" history of the system via $x_i^1(0)\ldots x_i^1(t-1)$ and $x_{cm}^j(0)\ldots x_{cm}^j(t-1)$.

Lemma 4. *For any agent r_i, $2\le j\le d$, any initial distribution $f_{x_i^j}(x;0)$ and any given* sample-paths $x_i^1(0)\ldots x_i^1(t-1)$, $x_{cm}^j(0)\ldots x_{cm}^j(t-1)$*; $f_{x_i^j}(x;t)$ pointwise converges to the normal distribution with mean $\bar{x}^j(t)$ and variance ${\sigma_i^j}^2(t)$, i.e. for large enough t we have*

$$f_{x_i^j}(x;t)\simeq\frac{1}{\sqrt{2\pi{\sigma_i^j}^2(t)}}\exp\left\{-\frac{(x-\bar{x}(t))^2}{2{\sigma_i^j}^2(t)}\right\} \tag{31}$$

$$\bar{x}^j(t)=\sum_{t'=0}^{t-1}\gamma\left(t'+1,t-1\right)\left(1-\alpha-\beta\rho_0x_i^1(t')\right)x_{cm}^j(t') \tag{32}$$

$${\sigma_i^j}^2(t)=\sigma_R^2\sum_{t'=0}^{t-1}\gamma^2\left(t'+1,t-1\right). \tag{33}$$

Proof. Recall that by the definitions of α and β the term $\alpha+\beta\rho_0x_i^1(t)$ is bounded by $\alpha\le\alpha+\beta\rho_0x_i^1(t)\le1-\alpha$. Hence for large enough t,

$$\gamma(0,t-1)=\prod_{t'=0}^{t-1}\left(\alpha+\beta\rho_0x_i^1(t')\right) \tag{34}$$
$$\le(1-\alpha)^t\simeq0 \tag{35}$$

hence $\varphi_{x_i^j}(\gamma(0,t-1)s;0)\simeq\varphi_{x_i^j}(0;0)=1$. Substitution of $\varphi_{x_i^j}(\gamma(0,t-1)s;0)\simeq1$ into Eq. (23) yields

$$\varphi_{x_i^j}(s;t)\simeq\prod_{t'=0}^{t-1}\exp\left\{\frac{1}{2}\sigma_R^2\gamma^2\left(t'+1,t-1\right)s^2\right\}\cdot\prod_{t'=0}^{t-1}\exp\left\{i\gamma\left(t'+1,t-1\right)s\left(1-\alpha-\beta\rho_0x_i^1(t')\right)x_{cm}^j(t')\right\} \tag{36}$$

$$=\exp\left\{\frac{1}{2}s^2\sigma_R^2\sum_{t'=0}^{t-1}\gamma^2\left(t'+1,t-1\right)\right\}+\exp\left\{is\sum_{t'=0}^{t-1}\gamma\left(t'+1,t-1\right)\left(1-\alpha-\beta\rho_0x_i^1(t')\right)x_{cm}^j(t')\right\} \tag{37}$$

$$=\exp\left\{is\bar{x}^j(t)+\frac{1}{2}s^2{\sigma_i^j}^2(t)\right\} \tag{38}$$

which is the characteristic function of the normal distribution with mean $\bar{x}^j(t)$ and variance ${\sigma_i^j}^2(t)$. $\bar{x}^j(t)$ and ${\sigma_i^j}^2(t)$ are defined above in Eqs. (32) and (33). □

We will say that the system has stabilized when the location distribution of all agents is close enough to the normal distribution described in Lemma 4. Denote by t_{stable} the stabilization time i.e. for every $t\ge t_{stable}$ the location distribution of all agents is as described in Lemma 4. We can not predict the agents' center of mass movement prior to stabilization. However, for every $t\ge t_{stable}$ the expected location of the center of mass is provided in the following lemma.

Lemma 5. *For every $t\ge t_{stable}$, any coordinate $2\le j\le d$ and any given* sample-paths $x_i^1(t_{stable})\ldots x_i^1(t-1)$, $x_{cm}^j(t_{stable})\ldots x_{cm}^j(t-1)$,

$$E\left[x_{cm}^j(t)\right]=\bar{x}^j(t)=\bar{x}^j(t_{stable}) \tag{39}$$

where the expectation is over the location of the agents at time t_{stable} and the set of random steps $R_1^j(t')\ldots R_M^j(t')$ for $t_{stable}\le t'\le t-1$.

Proof. By Lemma 4, for every $t \geq t_{stable}$ and any *sample-paths* $x_i^1(t_{stable})...x_i^1(t-1)$, $x_{cm}^j(t_{stable})...x_{cm}^j(t-1)$ we have $E[x_{cm}^j(t)] = \bar{x}^j(t)$. The second part of the lemma, i.e. $\bar{x}^j(t) = \bar{x}^j(t_{stable})$, is proved by induction on t. The induction base can be easily proved by substitution of $t = t_{stable}$ into Eq. (39). To prove the induction step, for every $t > t_{stable}$, assume that the induction hypothesis holds for $t-1$. Using Eq. (7), we write

$$x_{cm}^j(t) = \frac{1}{M}\sum_{i=1}^{M} x_i^j(t) \tag{40}$$

$$= x_{cm}^j(t-1) + \frac{1}{M}\sum_{i=1}^{M} R_1(t-1) - \frac{\beta\rho_0}{M}\sum_{i=1}^{M} x_i^1(t-1)\left(x_i^j(t-1) - x_{cm}^j(t-1)\right) \tag{41}$$

By performing expectation over both sides of the equation we get

$$E\left[x_{cm}^j(t)\right] = E\left[x_{cm}^j(t-1)\right] - \frac{\beta\rho_0}{M} E\left[\sum_{i=1}^{M} x_i^1(t-1)\left(x_i^j(t-1) - x_{cm}^j(t-1)\right)\right] \tag{42}$$

Using the induction hypothesis we have $E[x_{cm}^j(t-1)] = \bar{x}_{cm}^j(t-1) = \bar{x}_{cm}^j(t_{stable})$. The proof is concluded by showing that the second expected term of Eq. (42) equals zero. The second expected term can be evaluated by

$$E\left[\sum_{i=1}^{M} x_i^1(t')\left(x_i^j(t') - x_{cm}^j(t')\right)\right] = E_{x_{cm}^j(t'), x_i^j(t')}\left[\sum_{i=1}^{M} x_i^1(t')\left(x_i^j(t') - x_{cm}^j(t')\right) \,\middle|\, x_{cm}^j(t')\right] \tag{43}$$

$$= E_{x_{cm}^j(t')}\left[\sum_{i=1}^{M} x_i^1(t') \cdot E_{x_i^j(t')}\left[x_i^j(t') - x_{cm}^j(t') \mid x_{cm}^j(t')\right]\right] \tag{44}$$

where we have used the notation $t' = t-1$. We can further write

$$E_{x_i^j(t')}\left[x_i^j(t') - x_{cm}^j(t') \mid x_{cm}^j(t')\right] = \int_{-\infty}^{\infty} E_{x_i^j(t')}\left[x_i^j(t') - x_{cm}^j(t') \mid x_{cm}^j(t') = x\right] \cdot Pr\left[x_{cm}^j(t') = x\right] dx \tag{45}$$

Lemma 4 implies that the distributions of $x_i^j(t')$ and $x_{cm}^j(t')$ are symmetric around $\bar{x}^j(t')$ hence for all x, x' we have:

$$Pr\left[x_i^j(t') = \bar{x}^j(t') + x' \mid x_{cm}^j(t') = \bar{x}^j(t') + x\right] = Pr\left[x_i^j(t') = \bar{x}^j(t') - x' \mid x_{cm}^j(t') = \bar{x}^j(t') - x\right] \tag{46}$$

and

$$E_{x_i^j(t)}\left[x_i^j(t') - x_{cm}^j(t') \mid x_{cm}^j(t') = \bar{x}^j(t') + x\right]$$

$$= \int_{-\infty}^{\infty} (x' - x)\, Pr\left[x_i^j(t') = \bar{x}^j(t') + x' \mid x_{cm}^j(t') = \bar{x}^j(t') + x\right] dx' \tag{47}$$

$$= \int_{-\infty}^{\infty} (x' - x)\, Pr\left[x_i^j(t') = \bar{x}^j(t') - x' \mid x_{cm}^j(t') = \bar{x}^j(t') - x\right] dx' \tag{48}$$

$$= -\int_{-\infty}^{\infty} \left(\left(x_i^j(t') - x_{cm}^j(t')\right) \cdot Pr\left[x_i^j(t') = \bar{x}^j(t') - x' \mid x_{cm}^j(t') = \bar{x}^j(t') - x\right]\right) dx' \tag{49}$$

$$= -E\left[x_i^j(t') - x_{cm}^j(t') \mid x_{cm}^j(t') = \bar{x}^j(t') - x\right] \tag{50}$$

Finally, since $Pr[x_{cm}^j(t') = \bar{x}^j(t') + x] = Pr[x_{cm}^j(t') = \bar{x}^j(t') - x]$ the integrand of Eq. (45) is antisymmetric around $\bar{x}^j(t')$. Therefore the integral equals zero. $\square$

The following theorem concludes the correctness proof of the algorithm by stating that after stabilization the agents' center of mass travels at the direction of the gradient with a speed of at least $\beta\rho_0\sigma_R^2$ while not drifting toward any other directions.

Theorem 6. *For every $t \geq t_{stable}$ we have*

$$j = 1, \quad E\big[x^1_{cm}(t)\big] \geq x^1_{cm}(t_{stable}) + \beta\rho_0\sigma_R^2 \cdot (t - t_{stable}) \tag{51}$$

$$2 \leq j \leq d, \quad E\big[x^j_{cm}(t)\big] = \bar{x}^j(t_{stable}) \tag{52}$$

Proof. Eqs. (51) and (52) are restatements Lemmas 1 and 5 accordingly. □

4.2. Some reasonable approximations

Theorem 6 provides a lower bound on the speed of center of mass. The bound is not tight because the lower bound on the variance of the $j = 1$ coordinate of a single agent, provided in Lemma 2, is not tight. In this section, the variance of a single agent will be approximately computed using two relaxing assumptions. Note that the second assumption requires a large number of agents performing the algorithm ($M \gg 1$). The aim of the section is to provide intuition and insights into the workings of the algorithm hence a minimal M value is not provided and the assumptions are not proved but only justified.

The rule of motion, for the $j = 1$ coordinate can be written as

$$x^1_i(t+1) = x^1_i(t) + R^1_i(t) - \big(1 - \alpha - \beta\rho_0 x^1_{cm}(t)\big)\big(x^1_i(t) - x^1_{cm}(t)\big) + \beta\rho_0\big(x^1_i(t) - x^1_{cm}(t)\big)^2 \tag{53}$$

Since the swarm is cohesive, the term $x^1_i(t) - x^1_{cm}(t)$ is small. We relax the problem by neglecting the term quadratic in $x^1_i(t) - x^1_{cm}(t)$, yielding

$$x^1_i(t+1) \simeq x^1_i(t) + R^1_i(t) - \big(1 - \alpha - \beta\rho_0 x^1_{cm}(t)\big)\big(x^1_i(t) - x^1_{cm}(t)\big) \tag{54}$$

which is similar to the recursive equation for the $j \geq 2$ components with the term $x^1_i(t)$ replaced by $x^1_{cm}(t)$. The following lemma shows that the process described in Eq. (54) pointwise converges to the normal distribution with mean $\bar{x}^1(t)$ and variance $\sigma_i^{1^2}(t)$.

Lemma 7. *Given any initial distribution $f_{x^1_i}(x;0)$ and any given* sample-path $x^1_{cm}(0)\dots x^1_{cm}(t-1)$, *under the process described in Eq. (54), $f_{x^j_i}(x;t)$ pointwise converges to the normal distribution with mean $\bar{x}^1(t)$ and variance $\sigma^{1^2}(t)$, i.e. for large enough t we have*

$$f_{x^1_i}(x;t) \simeq \frac{1}{\sqrt{2\pi\sigma^{1^2}(t)}} \exp\left\{-\frac{(x - \bar{x}^1(t))^2}{2\sigma^{1^2}(t)}\right\} \tag{55}$$

where

$$\bar{x}^1(t) = \sum_{t'=0}^{t-1} \gamma\big(t'+1, t-1\big)\big(1 - \alpha - \beta\rho_0 x^1_{cm}(t')\big) x^1_{cm}(t') \tag{56}$$

$$\sigma^{1^2}(t) = \sigma_R^2 \sum_{t'=0}^{t-1} \gamma^2\big(t'+1, t-1\big) \tag{57}$$

$$\gamma(t_1, t_2) = \begin{cases} \prod_{t'=t_1}^{t_2} (\alpha + \beta\rho_0 x^1_{cm}(t')) & t_2 \geq t_1 \\ 1 & \text{else.} \end{cases} \tag{58}$$

Proof. Similarly to the proofs of Lemmas 3 and 4, the recursive equation for the characteristic function of $f_{x^1_i}(x;t)$ is given by

$$\varphi_{x^1_i}(s; t+1) = \varphi_{x^1_i}\big(\big(\alpha + \beta\rho_0 x^1_{cm}(t)\big)s; t\big) \cdot \varphi_R(s;t) \cdot \varphi_\delta(s;t) \tag{59}$$

The correctness of the following solution can be proved by induction on t,

$$\varphi_{x^1_i}(s;t) = \varphi_{x^1_i}\big(\gamma(0, t-1) \cdot s; 0\big) \cdot \prod_{t'=0}^{t-1} \exp\left\{\frac{1}{2}\sigma_R^2\gamma^2\big(t'+1, t-1\big)s^2\right\}$$
$$\cdot \prod_{t'=0}^{t-1} \exp\big\{i\gamma\big(t'+1, t-1\big)s\big(1 - \alpha - \beta\rho_0 x^1_{cm}(t')\big)x^1_{cm}(t')\big\} \tag{60}$$

For large enough t we have $\gamma(0,t) \simeq 0$ and

$$\varphi_{x_i^1}(s;t) \simeq \exp\left\{is\bar{x}^1(t) + \frac{1}{2}s^2{\sigma^1}^2(t)\right\} \tag{61}$$

which is the characteristic function of the normal distribution with mean $\bar{x}^1(t)$ and variance ${\sigma^1}^2(t)$. $\bar{x}^1(t)$ and ${\sigma^1}^2(t)$ are defined in the body of the lemma. □

Recall that we are interested in deriving the variance of $x_i^1(t)$. By Lemma 7,

$$Var\big[x_i^1(t)\big] = \sigma_1^2(t) \tag{62}$$

$$= \sigma_R^2 \sum_{t'=0}^{t-1}\left(\prod_{t''=t'+1}^{t-1}\big(\alpha + \beta\rho_0 x_{cm}^1(t'')\big)\right)^2 \tag{63}$$

By Eq. (63), the value of $Var[x_i^1(t)]$ is mostly dependent on the recent values of x_{cm}^1. Older x_{cm}^1 values have a negligible effect. Hence, by noting that the swarm's center of mass moves slowly in comparison to a single agent, we further relax the problem by assuming that for all t'', $x_{cm}^1(t'') = x_{cm}^1(t)$. Substitution of $x_{cm}^1(t'') = x_{cm}^1(t)$ into Eq. (63) yields

$$Var\big[x_i^1(t)\big] \simeq \sigma_R^2 \sum_{t'=0}^{t-1}\big(\alpha + \beta\rho_0 x_{cm}^1(t)\big)^{2t'} \tag{64}$$

$$= \sigma_R^2 \frac{1-(\alpha+\beta\rho_0 x_{cm}^1(t))^{2t}}{1-(\alpha+\beta\rho_0 x_{cm}^1(t))^2} \tag{65}$$

Considering large t we have

$$Var\big[x_i^1(t)\big] \simeq \frac{\sigma_R^2}{1-(\alpha+\beta\rho_0 x_{cm}^1(t))^2} \tag{66}$$

By substitution of Eq. (66) into Lemma 1 we get

$$E_{R(t)}\big[x_{cm}^1(t+1)\big] \simeq x_{cm}^1(t) + \frac{\beta\rho_0\sigma_R^2}{1-(\alpha+\beta\rho_0 x_{cm}^1(t))^2} \tag{67}$$

Note that the variance predicted by Eq. (66), is significantly larger than the variance previously provided by the lower bound, thus implying a faster drift with the gradient as can be seen in Eq. (67). Of course, the results of the approximate analysis also agree with the bound provided in Theorem 6.

5. Simulation and discussion

Extensive simulations with varying swarm sizes, parameters, and $\rho(\cdot)$ distributions were performed in order to verify the above presented analysis. In all experiments the agents successfully followed the gradient. For ease of viewing, only results of experiments performed in two-dimensional environments are presented.

The results of an experiment in a constant gradient field where $\nabla\rho = 0.01 \cdot \hat{x}^1$ are presented in Fig. 1. A snapshot of the agents distribution while executing the algorithm is presented in Fig. 1a. The marginal x^2 distribution was found to be normal as predicted by the analysis of Section 4.1. The marginal x^1 distribution was found to be in agreement with the approximate analysis of Section 4.2 i.e. normal distribution with the predicted variance. Recall that the marginal x^1 variance determines the speed of climbing the gradient hence it is important to evaluate it accurately.

The time courses of the two components of $X_{cm}(t)$ are presented in Fig. 1a. The swarm followed the gradient as expected i.e. the speed of drift toward $\hat{x}^1$ was as predicted by the approximate analysis of Section 4.2. The accurate estimation of the speed of drift further validates the two relaxing assumptions of Section 4.2. The small drift toward $\hat{x}^2$ is due to the random nature of the algorithm. According to the analysis, the swarm speed is independent of the number of agents executing the algorithm. Observe Fig. 2 for a comparison between several runs with varying swarm sizes. As expected, the drift speed was found to be identical for all swarm sizes.

Another issue to consider is group cohesiveness. According to the analysis, after stabilization, the location of every agent is distributed normally around $E[x_{cm}(t)]$. The variance of coordinate j of agent r_i was derived in Lemmas 4, 7 and was denoted by ${\sigma_i^j}^2(t)$. Hence group cohesiveness is characterized by the set of variances ${\sigma_i^j}^2(t)$. Unfortunately, each ${\sigma_i^j}^2(t)$ is determined by the history of the system via $x_i^1(0)\ldots x_i^1(t-1)$ and $x_{cm}^j(0)\ldots x_{cm}^j(t-1)$ hence can not be generally evaluated. Nevertheless, an upper bound on ${\sigma_i^j}^2(t)$ can be derived:

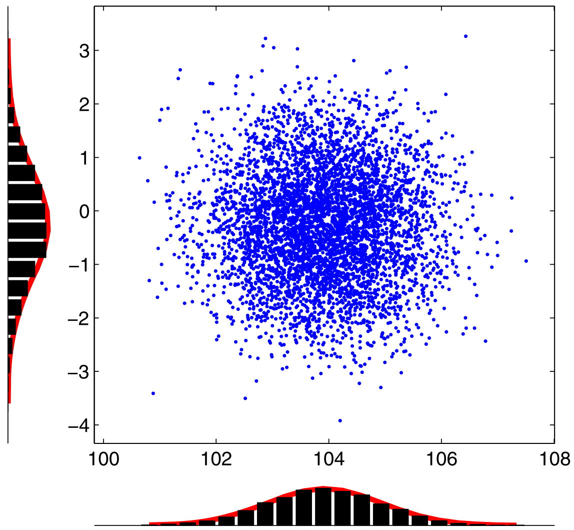

(a) A snapshot of the agents' distribution while executing the algorithm with the histograms of the marginal distributions for $\hat{x}^1$ and $\hat{x}^2$. The solid red lines are the predicted marginal distributions

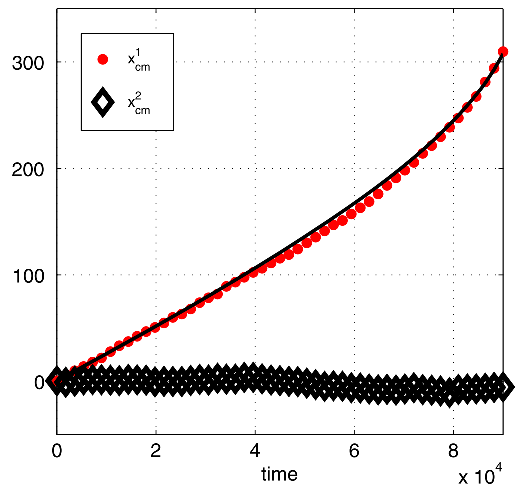

(b) The time course of the components x^1_{cm}, x^2_{cm} of X_{cm}. The solid lines are the theoretical predictions and the markers represent the actual results

Fig. 1. Results of a single simulation run of a swarm comprising 5000 agents with $\sigma_R^2 = 1$, $\alpha = 0.1$, $\beta = 0.25$. A constant gradient field was assumed i.e. $\rho(X) = 0.01 \cdot x^1$ ($\nabla\rho(X) = 0.01\hat{x}^1$).

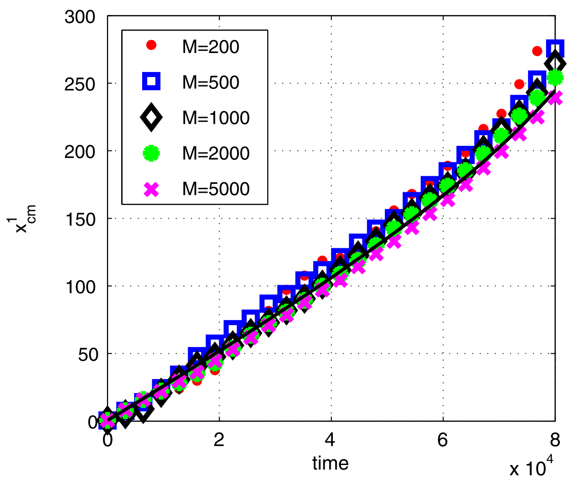

Fig. 2. Comparison between several swarm sizes where $\sigma_R^2 = 1$, $\alpha = 0.1$, $\beta = 0.25$ and $\rho(X) = 0.01 \cdot x^1$.

Corollary 8. *For any agent r_i, coordinate j and $t \geq t_{stable}$*

$$\sigma_i^{j^2}(t) \leq \frac{\sigma_R^2}{\alpha(2-\alpha)} \tag{68}$$

Proof. By Lemmas 4 and 7, we have:

$$\sigma_i^{j^2}(t) = \sigma_R^2 \sum_{t'=0}^{t-1} \gamma^2(t'+1, t-1) \tag{69}$$

$$\gamma(t_1, t_2) = \begin{cases} \prod_{t'=t_1}^{t_2} (\alpha + \beta\rho_0 x_i^1(t')) & t_2 \geq t_1 \\ 1 & \text{else} \end{cases} \tag{70}$$

Using $\alpha + \beta\rho_0 x_i^1(t') \leq 1 - \alpha$ we write $\gamma^2(t'+1, t-1) \leq (1-\alpha)^{2(t-t'-1)}$. Thus

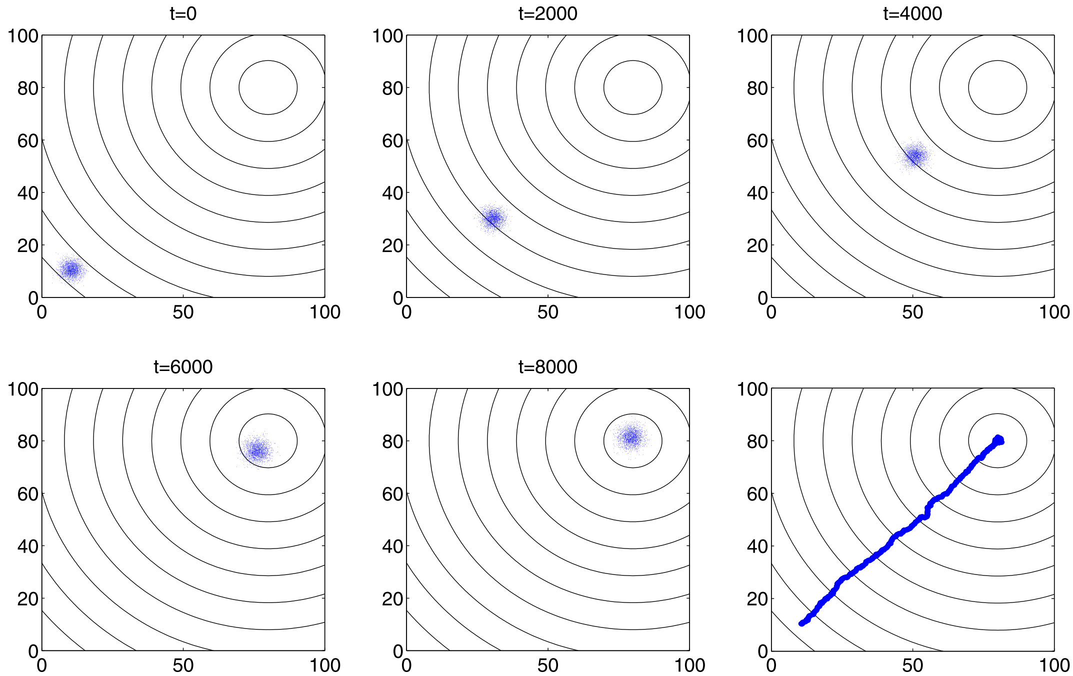

Fig. 3. Simulation in a simple environment. The contours represent the scalar field and the small dots are the agents. The path of the agents' center of mass is presented in the bottom right subfigure. In the experiment, the agents found the maxima and remained there.

$$\sigma_i^{j^2}(t) \le \sigma_R^2 \sum_{t'=0}^{t-1} (1-\alpha)^{2(t-t'-1)} \tag{71}$$

$$= \sigma_R^2 \frac{1-(1-\alpha)^{2t}}{1-(1-\alpha)^2} \tag{72}$$

$$\le \frac{\sigma_R^2}{\alpha(2-\alpha)}. \qquad \square \tag{73}$$

Group cohesiveness is especially important considering agents with limited sensing range. Using Corollary 8, the probability of any two agents being out of sensing range at any time $t \ge t_{stable}$ can be bounded. By properly setting the parameters σ_R^2 and α, the system can be designed to guarantee that all agent pairs will maintain sensing range with as high as required probability.

Recall that the algorithm was analyzed under the assumption that the gradient of $\rho(\cdot)$ is constant. The constant gradient assumption was justified by the small dimensions of the agents and the cohesiveness of the swarm: it is expected that the weak gradient of $\rho(\cdot)$ will be roughly constant in the small surroundings of the agents. Extensive simulations were performed in order to validate this assumption. It is important to keep in mind that the proposed algorithm is a gradient climbing algorithm hence cannot escape local maxima (as any other gradient climbing algorithm). Therefore, only environments with a single maximum were examined. In all experiments performed the agents successfully found the maximum of the signal. Observe Fig. 3 for the results of a simulation in a simple environment containing a single maximum. The path of the agents' center of mass is presented in the bottom right part of Fig. 3. The results of an experiment in a more intricate environment are presented in Fig. 4. In both environments $0 \le \rho(\cdot) \le 1$ and the algorithm parameters were: $M = 2000$, $\sigma_R^2 = 4$, $\alpha = 0.1$ and $\beta = 0.4$.

Simulations in noisy scalar fields were performed in order to examine the effects of noise on the algorithm. For example, two noisy scalar fields as well as the paths of the groups' center of masses are presented in Fig. 5. The noisy fields were created by adding normal white noise with standard deviation of 0.05 to the fields of Figs. 3 and 4. Recall that for the two non-noisy fields we have $0 \le \rho(\cdot) \le 1$ hence the amplitude of the noise is about 5% of the signal. In both runs, the swarm successfully followed the gradient and was unaffected by the noise, compare to Figs. 3 and 4. Note that the noise is fixed in place and time, hence, induces many local maxima. Generally, a gradient climbing algorithm cannot escape local maximas. However, since the algorithm "estimates" the gradient using sensor readings of agents spread in the environment, the swarm is able to escape these small local maxima.

An important issue to consider is robustness to failures. The algorithm is robust to clean failures i.e. agents that fail and completely vanish from the system. Furthermore, since the algorithm is memoryless, it is robust to all sorts of transient fail-

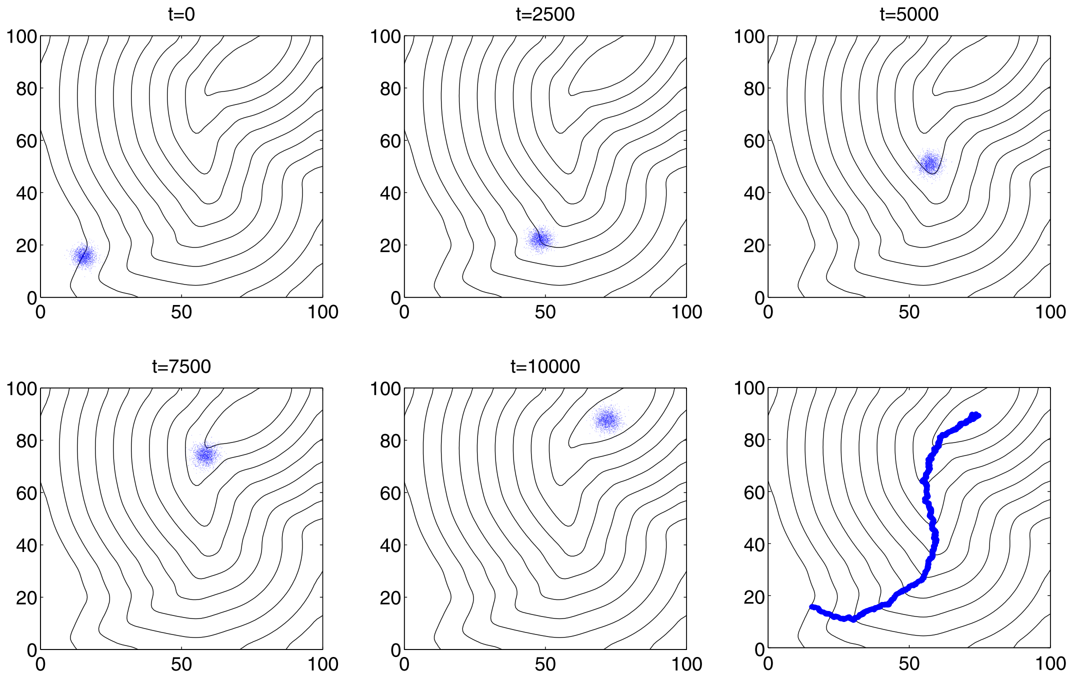

Fig. 4. Simulation in an intricate environment. The contours represent the scalar field and the small dots are the agents. The path of the agents' center of mass is presented in the bottom right subfigure. In the experiment, the agents found the maxima and remained there.

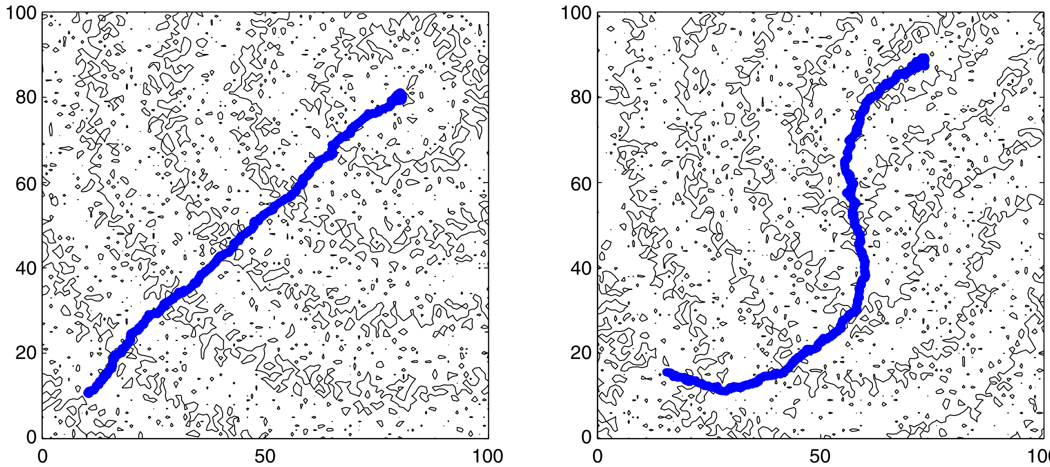

(a) The scalar field of Figure 3 with noise

(b) The scalar field of Figure 4 with noise

Fig. 5. The path of the agents' center of mass in two noisy environments. The variance of the noise is 5% of the signal.

ures i.e. agents that malfunction during a limited time span and resume normal behavior afterward. However, the algorithm fails when an agent is forced to remain stationary without vanishing from the system i.e., when the agent continue to exert attraction on all other agents. In that case, the stationary agent acts like an anchor preventing the swarm from following the gradient. We believe that robustness to such failures can be achieved using robust statistics. For example, at each time step, the center of mass will be derived excluding agents which are suspected of malfunctioning. The suspect agents are simply the agents which are far away from the rest of the swarm. Such robust algorithms worked well in simulation. We intend to further investigate this issue in the future.

5.1. Weaker sensing models

Up to this point, full mutual sensing of position was assumed. However, considering large groups, that assumption is not always feasible. In this section we will consider the weaker sensing model of full mutual sensing of directions i.e. every agent is able to sense the relative directions of all other agents but not their distance. Even tough sensing of direction only

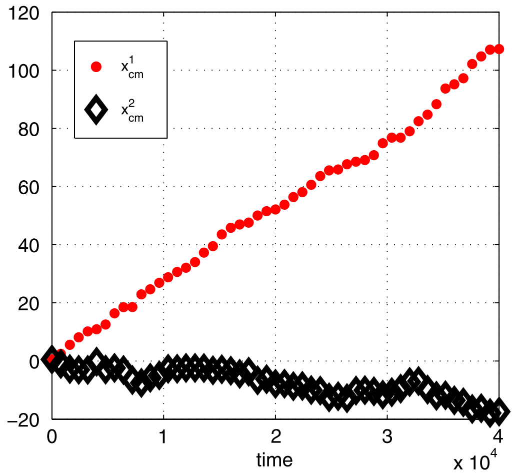

Fig. 6. The resulting time courses of the two components of $X_{cm}(t)$ of a single experiment using the motion rule of Eq. (76) in a two dimensional constant gradient field where $\rho(X) = 0.01 \cdot x^1$, $M = 500$, $\sigma_R^2 = 1$, $\alpha = 0.1$, $\beta = 0.25$.

is usually easier then full position sensing, full mutual sensing of direction is also not always feasible, the aim of this section is to demonstrate that our approach can be extended to other weaker sensing models.

Consider the following, slightly different, potential function and the gathering algorithm it implies

$$\tilde{\Psi} = \sum_{i,j} d(X_i, X_j) \tag{74}$$

$$\frac{\partial X_i}{\partial t} \triangleq -a\frac{\partial \tilde{\Psi}}{\partial t} = a\sum_j \frac{X_j - X_i}{d(X_i, X_j)} \tag{75}$$

Note that only full mutual sensing of directions is required in order to execute of the role of Eq. (75).

Based on the rule of motion of Eq. (75), we propose the following gradient climbing process:

$$X_i(t+1) = X_i(t) + R_i(t) + \bigl(1 - \alpha - \beta\rho(X_i)\bigr)\sum_j \frac{X_j - X_i}{d(X_i, X_j)} \tag{76}$$

In contradiction to the previously proposed rule, the size of the step here is independent of the distance to the center of mass but it is controlled by $\rho(\cdot)$. Compare the rule above to the rule proposed in Eq. (7).

Extensive simulations were performed to examine the behavior of the rule of motion above. In all experiments the swarm successfully followed the gradient. For example, the resulting time courses of the two components of $X_{cm}(t)$ of an experiment in a constant two dimensional gradient field are presented in Fig. 6. The swarm followed the gradient as expected. The small drift in $\hat{x}^2$ is due to the random nature of the algorithm.

6. Concluding remarks

In this paper a *reactive* gradient climbing algorithm for a large group of memoryless mobile robotic agents performing point measurements was presented. The proposed algorithm is based on a simple full mutual visibility gathering algorithm. We modified the speed with which the agents react to the “attraction forces” between them in order to indirectly cause the swarm drift in the direction of the gradient of ρ. In other words, the agents use indirect, motion-based communication, in order to implicitly “compare” their point measurements and follow the gradient. Furthermore, a random motion component was added in order to prevent gathering and allow sampling of the scalar field. We proved that the group follows the gradient cohesively under the assumption that the gradient is constant in the neighborhood spanned by the agents. We empirically demonstrated that the swarm indeed cohesively follows the gradient in complex and noisy scalar fields.

The algorithm was analyzed under the assumption of full mutual sensing of position. We have shown that the algorithm parameters can be tuned to guarantee that at (almost) all times, all agent pairs are close enough to allow mutual sensing. Furthermore, based on a gathering algorithm that requires mutual visibility of direction only we proposed and empirically evaluated a gradient following algorithm with the same sensing requirements. Since there are many gathering algorithms that require only local sensing (see e.g. [15,16]), an interesting open question is how can our approach be applied to enable gradient climbing with local sensing?

References

[1] Yotam Elor, Alfred M. Bruckstein, A thermodynamic approach to multi-robot cooperative localization, Theoret. Comput. Sci. 457 (0) (2012) 59–75.
[2] R.A. Russell, Robotic location of underground chemical sources, Robotica 22 (1) (2004) 109–115.
[3] E. Biyik, M. Arcak, Gradient climbing in formation via extremum seeking and passivity-based coordination rules, in: 46th IEEE Conf. on Decision and Control, 2007, pp. 3133–3138.
[4] J. Cochran, A. Siranosian, N. Ghods, M. Krstic, 3-d source seeking for underactuated vehicles without position measurement, IEEE Trans. Robot. 25 (1) (2009) 117–129.
[5] S. Liu, M. Krstic, Stochastic source seeking for nonholonomic unicycle, Automatica 46 (9) (2010) 1443–1453.
[6] A.S. Matveev, H. Teimoori, A.V. Savkin, Navigation of a unicycle-like mobile robot for environmental extremum seeking, Automatica 47 (1) (2011) 85–91.
[7] O. Khatib, Real-time obstacle avoidance for manipulators and mobile robots, Int. J. Robot. Res. 5 (1) (1986) 90–98.
[8] P. Ogren, E. Fiorelli, N.E. Leonard, Cooperative control of mobile sensor networks: adaptive gradient climbing in a distributed environment, IEEE Trans. Automat. Control 49 (8) (2004) 1292–1302.
[9] V. Gazi, K.M. Passino, Stability analysis of social foraging swarms, IEEE Trans. Syst. Man Cybern., Part B, Cybern. 34 (1) (2004) 539–557.
[10] B.J. Moore, C. Canudas de Wit, Source seeking via collaborative measurements by a circular formation of agents, in: American Control Conf., ACC, July 2010, pp. 6417–6422.
[11] Andrew Berdahl, Colin J. Torney, Christos C. Ioannou, Jolyon J. Faria, Iain D. Couzin, Emergent sensing of complex environments by mobile animal groups, Science 339 (6119) (2013) 574–576.
[12] Iain D. Couzin, Wencen Wu, Fumin Zhang, Bio-inspired source seeking with no explicit gradient estimation, in: Proc. IFAC Workshop on Distributed Estimation and Control in Networked System, 2012.
[13] Wencen Wu, Fumin Zhang, Robust cooperative exploration with a switching strategy, IEEE Trans. Robot. 28 (4) (2012) 828–839.
[14] Reuven Cohen, David Peleg, Robot convergence via center-of-gravity algorithms, in: Structural Information and Communication Complexity, in: Lecture Notes in Comput. Sci., vol. 3104, Springer, Berlin, Heidelberg, 2004, pp. 79–88.
[15] Noam Gordon, Yotam Elor, Alfred Bruckstein, Gathering multiple robotic agents with crude distance sensing capabilities, in: ANTS'08: Proceedings of the 6th International Conference on Ant Colony Optimization and Swarm Intelligence, Springer-Verlag, Berlin, Heidelberg, 2008, pp. 72–83.
[16] Paola Flocchini, Giuseppe Prencipe, Nicola Santoro, Peter Widmayer, Gathering of asynchronous oblivious robots with limited visibility, in: Afonso Ferreira, Horst Reichel (Eds.), STACS 2001, in: Lecture Notes in Comput. Sci., vol. 2010, Springer, Berlin, Heidelberg, 2001, pp. 247–258.